

Mass Corrections to the Vector Current Correlator[†]

K.G. Chetyrkin^{a,b}, R. Harlander^{c,‡}, J.H. Kühn^c and M. Steinhauser^a

^a*Max-Planck-Institut für Physik, Werner-Heisenberg-Institut,
D-80805 Munich, Germany*

^b*Institute for Nuclear Research, Russian Academy of Sciences,
Moscow 117312, Russia*

^c*Institut für Theoretische Teilchenphysik, Universität Karlsruhe,
D-76128 Karlsruhe, Germany.*

Abstract

Three-loop QCD corrections to the vector current correlator are considered. The large momentum procedure is applied in order to evaluate mass corrections up to order $(m^2/q^2)^6$. The inclusion of the first seven terms to the ratio $R = \sigma(e^+e^- \rightarrow \text{hadrons})/\sigma(e^+e^- \rightarrow \mu^+\mu^-)$ leads to reliable predictions from the high energy region down to relatively close to threshold.

PACS numbers: 12.38.-t, 12.38.Bx, 13.65.+i, 13.85.Lg.

*The complete postscript file of this preprint, including figures, is available via anonymous ftp at www-ttp.physik.uni-karlsruhe.de (129.13.102.139) as `/ttp97-11/ttp97-11.ps` or via www at <http://www-ttp.physik.uni-karlsruhe.de/cgi-bin/preprints>.

[†]Supported by BMBF under Contract 057KA92P, DFG under Contract Ku 502/8-1 and INTAS under Contract INTAS-93-744-ext.

[‡]Supported by the “Landesgraduiertenförderung” at the University of Karlsruhe.

1 Introduction

One of the most precise measurements of the strong coupling constant α_s is provided by the decay rate $\Gamma(Z \rightarrow \text{hadrons})$. In the high energy limit the quark masses may often be neglected. However, for precision measurements it is desirable to include also mass corrections of the form $(m^2/s)^l$ with $l = 1, 2, 3, \dots$. This is particularly valid if one wants to predict the total cross section for e^+e^- into hadrons in an energy region where s and m^2 are of comparable magnitude. In the massless limit corrections up to order α_s^3 are known [1, 2]. Terms of order $\alpha_s^2 m^2/s$, $\alpha_s^3 m^2/s$ [3, 4] and $\alpha_s^2 m^4/s^2$ [5] are also available at present, providing an acceptable approximation from the high energy region down to intermediate energy values. For the energy region closer to the production threshold terms of higher order in m^2/s are necessary. In this paper a systematic approach is presented to compute these terms. For the moment the vector current correlator only is considered. The starting point is thereby the polarization function $\Pi(q^2)$. With the method presented below we are able to evaluate the three-loop terms up to order $(m^2/q^2)^6$ in an expansion of $\Pi(q^2)$.

The polarization function $\Pi(q^2)$ is defined through

$$(-g_{\mu\nu}q^2 + q_\mu q_\nu) \Pi(q^2) = i \int dx e^{iqx} \langle 0 | T j_\mu(x) j_\nu(0) | 0 \rangle \quad (1)$$

and the physical observable $R(s)$ is related to $\Pi(q^2)$ by

$$R(s) = 12\pi \text{Im} \Pi(q^2 = s + i\epsilon). \quad (2)$$

It is convenient to write

$$\Pi(q^2) = \Pi^{(0)}(q^2) + \frac{\alpha_s(\mu^2)}{\pi} C_F \Pi^{(1)}(q^2) + \left(\frac{\alpha_s(\mu^2)}{\pi} \right)^2 \Pi^{(2)}(q^2) + \dots, \quad (3)$$

$$\Pi^{(2)} = C_F^2 \Pi_A^{(2)} + C_A C_F \Pi_{NA}^{(2)} + C_F T n_l \Pi_l^{(2)} + C_F T \Pi_F^{(2)}, \quad (4)$$

and similarly for $R(s)$. The colour factors ($C_F = (N_c^2 - 1)/(2N_c)$ and $C_A = N_c$) correspond to the Casimir operators of the fundamental and adjoint representations, respectively. For the numerical evaluation we set $N_c = 3$. The trace normalization of the fundamental representation is $T = 1/2$. The number of light (massless) quark flavours is denoted by n_l . In Eq. (4) $\Pi_A^{(2)}$ is the abelian contribution (quenched QED!) and $\Pi_{NA}^{(2)}$ is the non-abelian part specific for QCD. There are two fermionic contributions arising from double-bubble diagrams: For $\Pi_l^{(2)}$ the quark in the inner loop is massless, the external massive, whereas for $\Pi_F^{(2)}$ both fermions have the same mass. The result for $R_l^{(2)}(s)$ is known analytically [6] and will serve as check. The case where the external current couples to massless quarks and these via gluons to massive ones is treated in [7] and will not be addressed here.

The outline of the paper is as follows: In Sect. 2 we will describe the procedure which allows the systematic expansion for $\Pi(q^2)$ in analytic form for large external momentum and its implementation in a program. Sect. 3 contains the results separated according to the colour factors. In Sect. 4 the imaginary part of $\Pi(q^2)$ is considered and compared to the result of a recent evaluation using semi-analytical methods [8]. Finally the conclusions are presented in Sect. 5.

2 Large momentum procedure

In this section the basic rules of the large momentum procedure are briefly described and their implementation in programs is considered.

The methods which allow the expansion of Feynman diagrams containing either large masses (hard mass procedure) or large external momenta (large momentum procedure) have been used extensively in the recent past [9]. At one- and two-loop level it is in general still possible to perform the diagrammatic expansion “by hand” and only evaluate the integrals with algebraic programs. However, at three loops this is almost impossible, in particular if one is interested in an expansion up to high orders in m^2/s .

Following [10] the prescriptions for the expansion of an unrenormalized propagator type Feynman diagram in its large external momentum read:

1. Generate all subdiagrams of the initial graph such that
 - (a) they contain both vertices through which the large momentum enters and leaves the initial graph
 - (b) they become one-particle-irreducible when the two vertices are identified.
2. Taylor-expand the integrand of these subdiagrams in all small masses and external momenta generated by removing lines from the initial diagram.
3. In the initial diagram, shrink the subdiagram to a point and insert the result obtained from the expansion in 2.
4. Sum over all terms.

The subgraphs from step 1 are denoted *hard subgraphs* or simply *subgraphs*, the reduced graphs, resulting from step 3, the *co-subgraphs*.

For the non-planar three-loop topology all hard subgraphs are shown in Fig. 1. The corresponding co-subgraphs are obtained from the full graph by shrinking the displayed lines to a point. The number of terms generated by the large momentum procedure increases rapidly with the number of loops in the initial diagram. Also, the relation between the expansion momenta in the subgraph and the loop momenta of the co-subgraph becomes non-trivial. Nevertheless, the rules listed above provide an algorithm well suited for the evaluation through a computer. Restricting to three-loop two-point functions with large external momentum and an arbitrary number of small masses, the procedure was implemented using the language PERL. The program can be divided into the following steps:

1. (a) Generation of the relevant subgraphs and the corresponding co-subgraphs including the determination of their topologies, and
 - (b) distribution of momenta in the subgraph and co-subgraph respecting the relations between them.
2. Calculation of these terms.

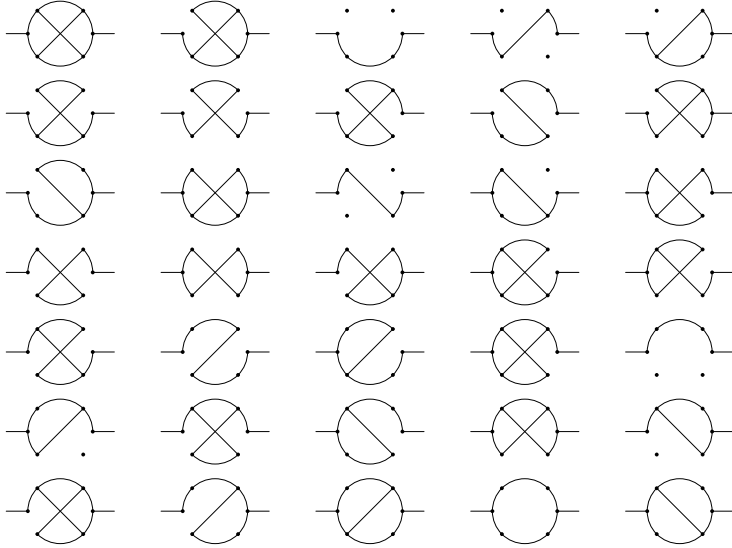


Figure 1: Possible topologies for the subgraphs of an NO-type diagram.

In step 1a, one only considers topologies, disregarding any properties of lines except their relative positions. Especially one neglects their momenta, masses, particle types, etc. For the representation of a diagram we label its vertices by integers and specify lines by their endpoints. A topology is thus described by the collection of its lines.

To generate the subdiagrams we first note that the full graph is always one of the hard subgraphs. The remaining ones are obtained by going through the following steps:

- (i) Remove any combination of lines from the initial diagram.
- (ii) Remove the emerging isolated dots and binary vertices.
- (iii) Relabel the remaining vertices by $\{1, \dots, \#\text{vertices}\}$ and build all permutations.
- (iv) Compare with a table listing the basic one- and two-loop topologies, assign the proper topology if it matches one of the entries or, otherwise, discard the result.

If a subgraph passes the last step, the corresponding co-subgraph is evidently fixed and its topology is determined in a similar way by applying steps (ii)-(iv). The result of this procedure is a database containing all relevant sub- and co-subgraphs, including information about their topology. Note that no selection criteria related to line properties have been applied so far. Thus, up to this point the procedure is universal and for each topology this part of the program has to be run only once and for all.

In step 1b, the database resulting from 1a is specialized to a specific diagram, including masses and momenta. The direction of the momentum carried by a line is connected with the order of the labels representing this line. Furthermore, for each subgraph the small

external momenta are routed in a way that they touch as few lines as possible. The output of step 1 is then the input for step 2, together with all the necessary administrative files like makefiles etc.

In step 2 the two FORM [11] packages MATAD and MINCER are used which were already available and have been applied to many different problems. MINCER [12] calculates massless three-loop propagator type integrals and therefore applies to the hard subgraphs. MATAD calculates massive tadpole diagrams up to three loops by using the corresponding recursion formulas obtained in [13] and is used for the co-subgraphs accordingly.

Allowing only for one internal mass scale m , the final result is then a power series in m^2/q^2 , where q is the (large) external momentum. The coefficient functions contain numerical constants together with $\ln^i(-q^2/m^2)$ and $\ln^j(-q^2/\mu^2)$ with $i \leq 3$ and $j \leq 2$, where μ is the renormalization scale.

3 Mass corrections to $\Pi(q^2)$

With the method presented in the previous section the first seven terms of the expansion have been computed. For the three-loop case 18 initial diagrams have to be considered. Altogether 240 subdiagrams are produced when the large momentum procedure is applied. The corresponding numbers in the two- (one-) loop case are 2 (1) initial and 14 (3) subdiagrams. The high energy approximation for $\Pi(q^2)$ reads in the $\overline{\text{MS}}$ scheme ($l_{qm} \equiv \ln(-q^2/\bar{m}^2)$, $l_{q\mu} \equiv \ln(-q^2/\mu^2)$):

$$\begin{aligned} \bar{\Pi}^{(0)} = & \frac{3}{16\pi^2} \left\{ \frac{20}{9} - \frac{4}{3} l_{q\mu} + 8 \frac{\bar{m}^2}{q^2} + \left(\frac{\bar{m}^2}{q^2} \right)^2 (4 + 8 l_{qm}) \right. \\ & + \left(\frac{\bar{m}^2}{q^2} \right)^3 \left(-\frac{64}{9} + \frac{32}{3} l_{qm} \right) + \left(\frac{\bar{m}^2}{q^2} \right)^4 (-22 + 24 l_{qm}) \\ & \left. + \left(\frac{\bar{m}^2}{q^2} \right)^5 \left(-\frac{992}{15} + 64 l_{qm} \right) + \left(\frac{\bar{m}^2}{q^2} \right)^6 \left(-\frac{1852}{9} + \frac{560}{3} l_{qm} \right) \right\} + \dots, \quad (5) \end{aligned}$$

$$\begin{aligned} \bar{\Pi}^{(1)} = & \frac{3}{16\pi^2} \left\{ \frac{55}{12} - 4 \zeta_3 - l_{q\mu} + \frac{\bar{m}^2}{q^2} (16 - 12 l_{q\mu}) \right. \\ & + \left(\frac{\bar{m}^2}{q^2} \right)^2 \left[\frac{2}{3} + 16 \zeta_3 + 22 l_{qm} - 24 l_{qm} l_{q\mu} + 12 l_{qm}^2 \right] \\ & + \left(\frac{\bar{m}^2}{q^2} \right)^3 \left[-\frac{736}{27} + \frac{1184}{27} l_{qm} + \frac{200}{9} l_{qm}^2 + (48 - 48 l_{qm}) l_{q\mu} \right] \\ & + \left(\frac{\bar{m}^2}{q^2} \right)^4 \left[-\frac{40313}{216} + \frac{1199}{9} l_{qm} + \frac{229}{3} l_{qm}^2 + (168 - 144 l_{qm}) l_{q\mu} \right] \\ & \left. + \left(\frac{\bar{m}^2}{q^2} \right)^5 \left[-\frac{2641601}{3375} + \frac{279196}{675} l_{qm} + \frac{12248}{45} l_{qm}^2 + (592 - 480 l_{qm}) l_{q\mu} \right] \right\} \end{aligned}$$

$$\begin{aligned}
& + \left(\frac{\bar{m}^2}{q^2} \right)^6 \left[-\frac{6117262}{2025} + \frac{184066}{135} l_{qm} + \frac{8992}{9} l_{qm}^2 \right. \\
& \quad \left. + (2132 - 1680 l_{qm}) l_{q\mu} \right] \} + \dots , \tag{6}
\end{aligned}$$

$$\begin{aligned}
\bar{\Pi}_A^{(2)} = & \frac{3}{16\pi^2} \left\{ -\frac{143}{72} - \frac{37}{6} \zeta_3 + 10 \zeta_5 + \frac{1}{8} l_{q\mu} \right. \\
& + \frac{\bar{m}^2}{q^2} \left[\frac{1667}{24} - \frac{5}{3} \zeta_3 - \frac{70}{3} \zeta_5 - \frac{51}{2} l_{q\mu} + 9 l_{q\mu}^2 \right] \\
& + \left(\frac{\bar{m}^2}{q^2} \right)^2 \left[\frac{127}{2} + 96 \zeta_3 - 48 \zeta_4 - 20 \zeta_5 + 8 B_4 + (36 + 24 \zeta_3) l_{qm} + \frac{33}{2} l_{qm}^2 \right. \\
& \quad \left. + 12 l_{qm}^3 + (31 - 48 \zeta_3 - 33 l_{qm} - 36 l_{qm}^2) l_{q\mu} + (-18 + 36 l_{qm}) l_{q\mu}^2 \right] \\
& + \left(\frac{\bar{m}^2}{q^2} \right)^3 \left[-\frac{177163}{2916} - 13 \zeta_3 - 64 \zeta_4 + \frac{320}{3} \zeta_5 + \frac{32}{3} B_4 \right. \\
& \quad + \left(\frac{9988}{81} + \frac{248}{3} \zeta_3 \right) l_{qm} + \frac{239}{3} l_{qm}^2 + \frac{2896}{81} l_{qm}^3 \\
& \quad \left. + \left(\frac{1750}{9} - \frac{410}{3} l_{qm} - 100 l_{qm}^2 \right) l_{q\mu} + (-144 + 108 l_{qm}) l_{q\mu}^2 \right] \\
& + \left(\frac{\bar{m}^2}{q^2} \right)^4 \left[-\frac{12656479}{15552} - \frac{14293}{54} \zeta_3 - 144 \zeta_4 + \frac{880}{3} \zeta_5 + 24 B_4 \right. \\
& \quad + \left(\frac{26783}{108} + \frac{826}{3} \zeta_3 \right) l_{qm} + \frac{494059}{1296} l_{qm}^2 + \frac{53701}{324} l_{qm}^3 \\
& \quad \left. + \left(\frac{48263}{36} - \frac{1765}{3} l_{qm} - 458 l_{qm}^2 \right) l_{q\mu} + (-612 + 432 l_{qm}) l_{q\mu}^2 \right] \\
& + \left(\frac{\bar{m}^2}{q^2} \right)^5 \left[-\frac{539215192817}{116640000} - \frac{1056859}{900} \zeta_3 - 384 \zeta_4 + \frac{3200}{3} \zeta_5 + 64 B_4 \right. \\
& \quad + \left(\frac{1191314219}{3240000} + \frac{14234}{15} \zeta_3 \right) l_{qm} + \frac{90647953}{54000} l_{qm}^2 + \frac{2940547}{4050} l_{qm}^3 \\
& \quad \left. + \left(\frac{328233}{50} - \frac{105554}{45} l_{qm} - \frac{6124}{3} l_{qm}^2 \right) l_{q\mu} + (-2580 + 1800 l_{qm}) l_{q\mu}^2 \right] \\
& + \left(\frac{\bar{m}^2}{q^2} \right)^6 \left[-\frac{420607059143}{19440000} - \frac{13059229}{2700} \zeta_3 - 1120 \zeta_4 + 4000 \zeta_5 + \frac{560}{3} B_4 \right. \\
& \quad + \left(\frac{133099291}{972000} + \frac{16842}{5} \zeta_3 \right) l_{qm} + \frac{54076013}{7200} l_{qm}^2 + \frac{8575579}{2700} l_{qm}^3 \\
& \quad + \left(\frac{13274779}{450} - \frac{142256}{15} l_{qm} - 8992 l_{qm}^2 \right) l_{q\mu} \\
& \quad \left. + (-10854 + 7560 l_{qm}) l_{q\mu}^2 \right] \} + \dots , \tag{7}
\end{aligned}$$

$$\begin{aligned}
\bar{\Pi}_{NA}^{(2)} = & \frac{3}{16\pi^2} \left\{ \frac{44215}{2592} - \frac{227}{18} \zeta_3 - \frac{5}{3} \zeta_5 + \left(-\frac{41}{8} + \frac{11}{3} \zeta_3 \right) l_{q\mu} + \frac{11}{24} l_{q\mu}^2 \right. \\
& + \frac{\bar{m}^2}{q^2} \left[\frac{1447}{24} + \frac{16}{3} \zeta_3 - \frac{85}{3} \zeta_5 - \frac{185}{6} l_{q\mu} + \frac{11}{2} l_{q\mu}^2 \right] \\
& + \left(\frac{\bar{m}^2}{q^2} \right)^2 \left[-\frac{5051}{216} + \frac{529}{9} \zeta_3 + 24 \zeta_4 - 30 \zeta_5 - 4 B_4 + \left(\frac{2123}{36} - 12 \zeta_3 \right) l_{q\mu} \right. \\
& \quad \left. + \frac{76}{3} l_{qm}^2 + \frac{11}{3} l_{qm}^3 + \left(-\frac{11}{18} - \frac{44}{3} \zeta_3 - \frac{105}{2} l_{qm} - 11 l_{qm}^2 \right) l_{q\mu} + 11 l_{qm} l_{q\mu}^2 \right] \\
& + \left(\frac{\bar{m}^2}{q^2} \right)^3 \left[-\frac{1278391}{11664} + \frac{149}{2} \zeta_3 + 32 \zeta_4 - \frac{80}{3} \zeta_5 - \frac{16}{3} B_4 \right. \\
& \quad + \left(\frac{247627}{1944} - \frac{158}{3} \zeta_3 \right) l_{qm} + \frac{745}{18} l_{qm}^2 + \frac{352}{81} l_{qm}^3 \\
& \quad \left. + \left(\frac{7262}{81} - \frac{8494}{81} l_{qm} - \frac{550}{27} l_{qm}^2 \right) l_{q\mu} + (-22 + 22 l_{qm}) l_{q\mu}^2 \right] \\
& + \left(\frac{\bar{m}^2}{q^2} \right)^4 \left[-\frac{13377061}{31104} + \frac{4840}{27} \zeta_3 + 72 \zeta_4 - \frac{220}{3} \zeta_5 - 12 B_4 \right. \\
& \quad + \left(\frac{1154479}{2592} - \frac{512}{3} \zeta_3 \right) l_{qm} + \frac{98381}{648} l_{qm}^2 + \frac{973}{81} l_{qm}^3 \\
& \quad \left. + \left(\frac{1030099}{2592} - \frac{34141}{108} l_{qm} - \frac{2519}{36} l_{qm}^2 \right) l_{q\mu} + (-77 + 66 l_{qm}) l_{q\mu}^2 \right] \\
& + \left(\frac{\bar{m}^2}{q^2} \right)^5 \left[-\frac{418731949411}{233280000} + \frac{335497}{600} \zeta_3 + 192 \zeta_4 - \frac{800}{3} \zeta_5 - 32 B_4 \right. \\
& \quad + \left(\frac{5920594861}{3888000} - \frac{2863}{5} \zeta_3 \right) l_{qm} + \frac{1433459}{2400} l_{qm}^2 + \frac{14063}{324} l_{qm}^3 \\
& \quad \left. + \left(\frac{61358611}{40500} - \frac{2077289}{2025} l_{qm} - \frac{33682}{135} l_{qm}^2 \right) l_{q\mu} + \left(-\frac{814}{3} + 220 l_{qm} \right) l_{q\mu}^2 \right] \\
& + \left(\frac{\bar{m}^2}{q^2} \right)^6 \left[-\frac{34153293329}{4665600} + \frac{902921}{450} \zeta_3 + 560 \zeta_4 - 1000 \zeta_5 - \frac{280}{3} B_4 \right. \\
& \quad + \left(\frac{49904336431}{9720000} - 1988 \zeta_3 \right) l_{qm} + \frac{50112223}{21600} l_{qm}^2 + \frac{1376567}{8100} l_{qm}^3 \\
& \quad + \left(\frac{34271558}{6075} - \frac{2845663}{810} l_{qm} - \frac{24728}{27} l_{qm}^2 \right) l_{q\mu} \\
& \quad \left. + \left(-\frac{5863}{6} + 770 l_{qm} \right) l_{q\mu}^2 \right] \left. \right\} + \dots , \tag{8}
\end{aligned}$$

$$\begin{aligned}
\bar{\Pi}_l^{(2)} = & \frac{3}{16\pi^2} \left\{ -\frac{3701}{648} + \frac{38}{9} \zeta_3 + \left(\frac{11}{6} - \frac{4}{3} \zeta_3 \right) l_{q\mu} - \frac{1}{6} l_{q\mu}^2 \right. \\
& \left. + \frac{\bar{m}^2}{q^2} \left[-\frac{95}{6} + \frac{26}{3} l_{q\mu} - 2 l_{q\mu}^2 \right] \right\}
\end{aligned}$$

$$\begin{aligned}
& + \left(\frac{\bar{m}^2}{q^2} \right)^2 \left[-\frac{83}{54} - \frac{224}{9} \zeta_3 - \frac{145}{9} l_{qm} - \frac{20}{3} l_{qm}^2 - \frac{4}{3} l_{qm}^3 \right. \\
& \quad \left. + \left(\frac{2}{9} + \frac{16}{3} \zeta_3 + 14 l_{qm} + 4 l_{qm}^2 \right) l_{q\mu} - 4 l_{qm} l_{q\mu}^2 \right] \\
& + \left(\frac{\bar{m}^2}{q^2} \right)^3 \left[\frac{1292}{729} - \frac{128}{9} \zeta_3 - \frac{11182}{243} l_{qm} - \frac{344}{27} l_{qm}^2 - \frac{128}{81} l_{qm}^3 \right. \\
& \quad \left. + \left(-\frac{1816}{81} + \frac{2264}{81} l_{qm} + \frac{200}{27} l_{qm}^2 \right) l_{q\mu} + (8 - 8 l_{qm}) l_{q\mu}^2 \right] \\
& + \left(\frac{\bar{m}^2}{q^2} \right)^4 \left[\frac{11941}{144} - 8 \zeta_3 - \frac{42641}{324} l_{qm} - \frac{4883}{108} l_{qm}^2 - \frac{127}{27} l_{qm}^3 \right. \\
& \quad \left. + \left(-\frac{70553}{648} + \frac{2279}{27} l_{qm} + \frac{229}{9} l_{qm}^2 \right) l_{q\mu} + (28 - 24 l_{qm}) l_{q\mu}^2 \right] \\
& + \left(\frac{\bar{m}^2}{q^2} \right)^5 \left[\frac{391086983}{911250} + \frac{448}{45} \zeta_3 - \frac{2461553}{6075} l_{qm} - \frac{113648}{675} l_{qm}^2 - \frac{6488}{405} l_{qm}^3 \right. \\
& \quad \left. + \left(-\frac{4306601}{10125} + \frac{549196}{2025} l_{qm} + \frac{12248}{135} l_{qm}^2 \right) l_{q\mu} + \left(\frac{296}{3} - 80 l_{qm} \right) l_{q\mu}^2 \right] \\
& + \left(\frac{\bar{m}^2}{q^2} \right)^6 \left[\frac{165619333}{91125} + \frac{2432}{27} \zeta_3 - \frac{1763021}{1350} l_{qm} - \frac{51451}{81} l_{qm}^2 - \frac{4664}{81} l_{qm}^3 \right. \\
& \quad \left. + \left(-\frac{9715012}{6075} + \frac{373066}{405} l_{qm} + \frac{8992}{27} l_{qm}^2 \right) l_{q\mu} \right. \\
& \quad \left. + \left(\frac{1066}{3} - 280 l_{qm} \right) l_{q\mu}^2 \right] \} + \dots, \tag{9}
\end{aligned}$$

$$\begin{aligned}
\bar{\Pi}_F^{(2)} & = \frac{3}{16\pi^2} \left\{ -\frac{3701}{648} + \frac{38}{9} \zeta_3 + \left(\frac{11}{6} - \frac{4}{3} \zeta_3 \right) l_{q\mu} - \frac{1}{6} l_{q\mu}^2 \right. \\
& \quad \left. + \frac{\bar{m}^2}{q^2} \left[-\frac{223}{6} + 16 \zeta_3 + \frac{26}{3} l_{q\mu} - 2 l_{q\mu}^2 \right] \right. \\
& \quad + \left(\frac{\bar{m}^2}{q^2} \right)^2 \left[-\frac{1505}{54} + \frac{352}{9} \zeta_3 + \left(-\frac{439}{9} + 8 \zeta_3 \right) l_{qm} - \frac{23}{3} l_{qm}^2 - \frac{4}{3} l_{qm}^3 \right. \\
& \quad \left. + \left(\frac{2}{9} + \frac{16}{3} \zeta_3 + 14 l_{qm} + 4 l_{qm}^2 \right) l_{q\mu} - 4 l_{qm} l_{q\mu}^2 \right] \\
& \quad + \left(\frac{\bar{m}^2}{q^2} \right)^3 \left[\frac{69374}{729} + \frac{1120}{27} \zeta_3 - \frac{6050}{81} l_{qm} - \frac{436}{81} l_{qm}^2 - \frac{112}{81} l_{qm}^3 \right. \\
& \quad \left. + \left(-\frac{1816}{81} + \frac{2264}{81} l_{qm} + \frac{200}{27} l_{qm}^2 \right) l_{q\mu} + (8 - 8 l_{qm}) l_{q\mu}^2 \right] \\
& \quad + \left(\frac{\bar{m}^2}{q^2} \right)^4 \left[\frac{175813}{432} + 186 \zeta_3 - \frac{87737}{324} l_{qm} - \frac{8501}{108} l_{qm}^2 - \frac{370}{27} l_{qm}^3 \right. \\
& \quad \left. + \left(-\frac{70553}{648} + \frac{2279}{27} l_{qm} + \frac{229}{9} l_{qm}^2 \right) l_{q\mu} + (28 - 24 l_{qm}) l_{q\mu}^2 \right]
\end{aligned}$$

$$\begin{aligned}
& + \left(\frac{\bar{m}^2}{q^2} \right)^5 \left[\frac{843731341}{455625} + \frac{84064}{135} \zeta_3 - \frac{5236781}{10125} l_{qm} - \frac{646424}{2025} l_{qm}^2 - \frac{8072}{81} l_{qm}^3 \right. \\
& \quad \left. + \left(-\frac{4306601}{10125} + \frac{549196}{2025} l_{qm} + \frac{12248}{135} l_{qm}^2 \right) l_{q\mu} + \left(\frac{296}{3} - 80 l_{qm} \right) l_{q\mu}^2 \right] \\
& + \left(\frac{\bar{m}^2}{q^2} \right)^6 \left[\frac{2624352259}{364500} + \frac{41212}{27} \zeta_3 + \frac{3852533}{24300} l_{qm} - \frac{34499}{54} l_{qm}^2 - \frac{18142}{27} l_{qm}^3 \right. \\
& \quad \left. + \left(-\frac{9715012}{6075} + \frac{373066}{405} l_{qm} + \frac{8992}{27} l_{qm}^2 \right) l_{q\mu} \right. \\
& \quad \left. + \left(\frac{1066}{3} - 280 l_{qm} \right) l_{q\mu}^2 \right] \} + \dots , \tag{10}
\end{aligned}$$

where \bar{m} is the $\overline{\text{MS}}$ renormalized mass at scale μ^2 and ζ is Riemann's zeta-function with the values $\zeta_2 = \pi^2/6$, $\zeta_3 \approx 1.20206$, $\zeta_4 = \pi^4/90$ and $\zeta_5 \approx 1.03693$. B_4 is a constant typical for massive three-loop integrals with $B_4 = -\frac{13}{2}\zeta_4 - 4\zeta_2 \ln^2 2 + \frac{2}{3} \ln^4 2 + 16\text{Li}_4(\frac{1}{2}) \approx -1.762800$ [13]. The overall renormalization of $\bar{\Pi}(q^2)$ is also performed in the $\overline{\text{MS}}$ scheme, i.e. in the expressions obtained after renormalization of m and α_s only the poles are subtracted. The expressions renormalized in the conventional QED scheme are obtained by subtracting $\bar{\Pi}(0)$ given e.g. in [13, 8] in order to obtain $\Pi(0) = 0$. The $(m^2/q^2)^2$ terms in the case of QED can also be found in [14].

4 $\sigma(e^+e^- \rightarrow \text{hadrons})$

According to Eq. (2) the ratio $R(s)$ is obtained by taking the imaginary part arising from the $\ln(-q^2)$ terms of the above results. Note that starting from the quartic term logarithms in the mass \bar{m} appear which cannot be removed by a choice of the renormalization scale μ . A closer look into the method used for the calculation shows that starting from this order massive tadpoles appear, these being the source for such logarithms in agreement with the general discussion of [15, 16]. For $\mu^2 = s$ which is the natural scale at high energies, the $(\bar{m}^2/s)^0$ and $(\bar{m}^2/s)^1$ terms are free of logarithms. We refrain from listing the corresponding results which are trivially obtained from Eqs.(5)-(10).

Using the relation between the $\overline{\text{MS}}$ and the on-shell mass [17] leads to the ratio $R(s)$ expressed in terms of the pole mass ($L_{ms} \equiv \ln(m^2/s)$, $L_{s\mu} \equiv \ln(s/\mu^2)$):

$$\begin{aligned}
R^{(0)} = & 3 \left\{ 1 - 6 \left(\frac{m^2}{s} \right)^2 - 8 \left(\frac{m^2}{s} \right)^3 - 18 \left(\frac{m^2}{s} \right)^4 - 48 \left(\frac{m^2}{s} \right)^5 \right. \\
& \left. - 140 \left(\frac{m^2}{s} \right)^6 \right\} + \dots , \tag{11}
\end{aligned}$$

$$\begin{aligned}
R^{(1)} = & 3 \left\{ \frac{3}{4} + 9 \frac{m^2}{s} + \left(\frac{m^2}{s} \right)^2 \left[\frac{15}{2} - 18L_{ms} \right] + \left(\frac{m^2}{s} \right)^3 \left[-\frac{188}{9} - \frac{116}{3}L_{ms} \right] \right. \\
& \left. + \left(\frac{m^2}{s} \right)^4 \left[-\frac{983}{12} - \frac{203}{2}L_{ms} \right] + \left(\frac{m^2}{s} \right)^5 \left[-\frac{61699}{225} - \frac{4676}{15}L_{ms} \right] \right\}
\end{aligned}$$

$$+ \left(\frac{m^2}{s}\right)^6 \left[-\frac{84743}{90} - \frac{3064}{3}L_{ms} \right] \} + \dots, \quad (12)$$

$$\begin{aligned} R_A^{(2)} = & 3 \left\{ -\frac{3}{32} + \frac{m^2}{s} \left[\frac{9}{8} + \frac{27}{2}L_{ms} \right] \right. \\ & + \left(\frac{m^2}{s}\right)^2 \left[-\frac{345}{16} + (99 - 72 \ln 2) \zeta_2 + 36 \zeta_3 + \frac{81}{4}L_{ms} - 27L_{ms}^2 \right] \\ & + \left(\frac{m^2}{s}\right)^3 \left[\frac{12469}{216} + \left(\frac{2582}{9} - 144 \ln 2\right) \zeta_2 - 26 \zeta_3 - \frac{139}{2}L_{ms} - \frac{886}{9}L_{ms}^2 \right] \\ & + \left(\frac{m^2}{s}\right)^4 \left[\frac{6551}{72} + \left(\frac{64717}{72} - 432 \ln 2\right) \zeta_2 - \frac{197}{2} \zeta_3 - \frac{360005}{864}L_{ms} \right. \\ & \quad \left. - \frac{45277}{144}L_{ms}^2 \right] \\ & + \left(\frac{m^2}{s}\right)^5 \left[\frac{259771381}{4320000} + \left(\frac{2773147}{900} - 1440 \ln 2\right) \zeta_2 - \frac{3517}{10} \zeta_3 \right. \\ & \quad \left. - \frac{63112847}{36000}L_{ms} - \frac{1963147}{1800}L_{ms}^2 \right] \\ & + \left(\frac{m^2}{s}\right)^6 \left[-\frac{748405531}{1296000} + \left(\frac{6599179}{600} - 5040 \ln 2\right) \zeta_2 - \frac{12663}{10} \zeta_3 \right. \\ & \quad \left. - \frac{33526867}{4800}L_{ms} - \frac{4709179}{1200}L_{ms}^2 \right] \} + \dots, \quad (13) \end{aligned}$$

$$\begin{aligned} R_{NA}^{(2)} = & 3 \left\{ \frac{123}{32} - \frac{11}{4} \zeta_3 - \frac{11}{16}L_{s\mu} + \frac{m^2}{s} \left[\frac{185}{8} - \frac{33}{4}L_{s\mu} \right] \right. \\ & + \left(\frac{m^2}{s}\right)^2 \left[\frac{77}{3} + \left(\frac{9}{2} + 36 \ln 2\right) \zeta_2 + 11 \zeta_3 \right. \\ & \quad \left. - \frac{381}{8}L_{ms} + \frac{33}{4}L_{ms}^2 + \left(-\frac{55}{8} + \frac{33}{2}L_{ms}\right) L_{s\mu} \right] \\ & + \left(\frac{m^2}{s}\right)^3 \left[-\frac{61951}{2592} + \left(\frac{26}{9} + 72 \ln 2\right) \zeta_2 + \frac{43}{2} \zeta_3 \right. \\ & \quad \left. - \frac{11779}{108}L_{ms} + 22L_{ms}^2 + \left(\frac{517}{27} + \frac{319}{9}L_{ms}\right) L_{s\mu} \right] \\ & + \left(\frac{m^2}{s}\right)^4 \left[-\frac{372361}{1728} + \left(-\frac{2579}{72} + 216 \ln 2\right) \zeta_2 + 74 \zeta_3 \right. \\ & \quad \left. - \frac{61961}{216}L_{ms} + \frac{10793}{144}L_{ms}^2 + \left(\frac{10813}{144} + \frac{2233}{24}L_{ms}\right) L_{s\mu} \right] \\ & + \left(\frac{m^2}{s}\right)^5 \left[-\frac{4611741517}{5184000} + \left(-\frac{63869}{360} + 720 \ln 2\right) \zeta_2 + \frac{4989}{20} \zeta_3 \right. \end{aligned}$$

$$\begin{aligned}
& -\frac{34493231}{43200}L_{ms} + \frac{20357}{80}L_{ms}^2 + \left(\frac{678689}{2700} + \frac{12859}{45}L_{ms}\right)L_{s\mu} \Big] \\
& + \left(\frac{m^2}{s}\right)^6 \left[-\frac{13915043077}{4320000} + \left(-\frac{1316833}{1800} + 2520 \ln 2\right)\zeta_2 + 861\zeta_3 \right. \\
& \left. -\frac{103349851}{43200}L_{ms} + \frac{1058411}{1200}L_{ms}^2 + \left(\frac{932173}{1080} + \frac{8426}{9}L_{ms}\right)L_{s\mu} \right] \Big\} + \dots, \tag{14}
\end{aligned}$$

$$\begin{aligned}
R_l^{(2)} = & 3 \left\{ -\frac{11}{8} + \zeta_3 + \frac{1}{4}L_{s\mu} + \frac{m^2}{s} \left[-\frac{13}{2} + 3L_{s\mu} \right] \right. \\
& + \left(\frac{m^2}{s}\right)^2 \left[-\frac{35}{6} - 18\zeta_2 - 4\zeta_3 + \frac{27}{2}L_{ms} - 3L_{ms}^2 + \left(\frac{5}{2} - 6L_{ms}\right)L_{s\mu} \right] \\
& + \left(\frac{m^2}{s}\right)^3 \left[\frac{1282}{81} - \frac{304}{9}\zeta_2 + \frac{752}{27}L_{ms} - 8L_{ms}^2 + \left(-\frac{188}{27} - \frac{116}{9}L_{ms}\right)L_{s\mu} \right] \\
& + \left(\frac{m^2}{s}\right)^4 \left[\frac{7091}{96} - \frac{260}{3}\zeta_2 + \frac{5291}{72}L_{ms} - \frac{53}{2}L_{ms}^2 + \left(-\frac{983}{36} - \frac{203}{6}L_{ms}\right)L_{s\mu} \right] \\
& + \left(\frac{m^2}{s}\right)^5 \left[\frac{2712517}{10125} - \frac{11872}{45}\zeta_2 \right. \\
& \quad \left. + \frac{142327}{675}L_{ms} - 92L_{ms}^2 + \left(-\frac{61699}{675} - \frac{4676}{45}L_{ms}\right)L_{s\mu} \right] \\
& + \left(\frac{m^2}{s}\right)^6 \left[\frac{15168713}{16200} - \frac{7744}{9}\zeta_2 \right. \\
& \quad \left. + \frac{9721}{15}L_{ms} - \frac{2972}{9}L_{ms}^2 + \left(-\frac{84743}{270} - \frac{3064}{9}L_{ms}\right)L_{s\mu} \right] \Big\} + \dots, \tag{15}
\end{aligned}$$

$$\begin{aligned}
R_F^{(2)} = & 3 \left\{ -\frac{11}{8} + \zeta_3 + \frac{1}{4}L_{s\mu} + \frac{m^2}{s} \left[-\frac{13}{2} + 3L_{s\mu} \right] \right. \\
& + \left(\frac{m^2}{s}\right)^2 \left[\frac{2}{3} + 18\zeta_2 - 10\zeta_3 + 12L_{ms} - 3L_{ms}^2 + \left(\frac{5}{2} - 6L_{ms}\right)L_{s\mu} \right] \\
& + \left(\frac{m^2}{s}\right)^3 \left[\frac{4}{3} + \frac{352}{9}\zeta_2 + \frac{350}{9}L_{ms} - \frac{76}{9}L_{ms}^2 + \left(-\frac{188}{27} - \frac{116}{9}L_{ms}\right)L_{s\mu} \right] \\
& + \left(\frac{m^2}{s}\right)^4 \left[\frac{20233}{288} + \frac{533}{6}\zeta_2 + \frac{1673}{72}L_{ms} - \frac{25}{4}L_{ms}^2 \right. \\
& \quad \left. + \left(-\frac{983}{36} - \frac{203}{6}L_{ms}\right)L_{s\mu} \right] \\
& + \left(\frac{m^2}{s}\right)^5 \left[-\frac{54559}{6750} + \frac{3592}{45}\zeta_2 - \frac{1157}{75}L_{ms} + \frac{4328}{45}L_{ms}^2 \right. \\
& \quad \left. + \left(-\frac{61699}{675} - \frac{4676}{45}L_{ms}\right)L_{s\mu} \right]
\end{aligned}$$

$$\begin{aligned}
& + \left(\frac{m^2}{s}\right)^6 \left[-\frac{9214697}{6480} - 1105 \zeta_2 + \frac{346981}{540} L_{ms} + \frac{18937}{18} L_{ms}^2 \right. \\
& \quad \left. + \left(-\frac{84743}{270} - \frac{3064}{9} L_{ms} \right) L_{s\mu} \right] \} + \dots \quad (16)
\end{aligned}$$

The quartic terms are in agreement with the results of [5]. For the contribution containing massless fermions, $R_l^{(2)}$, a comparison with the full analytical result is possible [6]. We found complete agreement up to the order considered.

The results of the expansion can now be compared with those obtained via a semi-analytical procedure using the method of conformal mapping and Padé approximation [8] which are valid in the whole energy range. To conform with the conventions of [8], $\mu^2 = m^2$ has been adopted for this comparison. In Fig. 2 successively higher orders in (m^2/s) are included (dashed lines) and compared with the Padé result (narrow dots). By comparing the quadratic approximation with the one containing also terms of order $(m^2/s)^6$ (solid line) one observes that the quality of the approximation improves considerably.

For completeness we also present in Figs. 3 the results for the scale $\mu^2 = s$. This choice is more adequate to the high energy region and all functions $R_i, i = A, NA, l, F$ approach the constants to be read off easily from Eqs.(13)-(16).

Let us discuss separately the high energy and the low energy regions. For all three functions R_A, R_{NA} and R_l and values between $x = 0$ and $x = 0.6$ ($x = 2m/\sqrt{s}$) the expansions including terms of order $(m^2/s)^3$ (or more) are in perfect agreement with the semi-analytical result. Conversely this provides a completely independent test of the method of [8] which did rely mainly on low energy information. Including more terms in the expansion, one obtains an improved approximation even in the low energy region. However, the quality of the “convergence” is significantly better for R_l and R_{NA} than for R_A . Two reasons may be responsible for this difference: (i) In a high energy expansion it is presumably more difficult to approximate the $1/v$ Coulomb singularity in R_A than the mild $\ln v$ singularity in R_{NA} and R_l . (ii) The function R_l can be approximated in the whole energy region $2m < \sqrt{s} < \infty$ by an increasing number of terms with arbitrary accuracy. This is evident from the known analytical form of R_l , a consequence of the absence of thresholds above $2m$ in this piece. In contrast the functions R_A and R_{NA} exhibit a four particle threshold at $\sqrt{s} = 4m$. The high energy expansion is, therefore, not expected to converge to the correct answer in the interval between $2m$ and $4m$. For R_{NA} this feature can be studied in more detail by separating R_{NA} into the gluonic double-bubble terms in the $\xi = 4$ gauge [18] and a remainder. This separation is possible both for the semi-analytical result and the expansion (Fig. 4). The remainder approaches a constant both for $x \rightarrow 0$ and $x \rightarrow 1$. For $0 < x < 0.5$ the agreement is perfect. It extends even up to $x \approx 0.9$, a fact which is quite remarkable and surprising.

For R_F the expansion is also shown in Fig. 2. Again one observes quick convergence for x between 0 and 0.5. No (semi-)analytical result is available for the comparison with R_F . However, in the region below the four particle threshold an analytical result is available, based on the calculation of the form factor in [6]. The four fermion contribution is expected to be small for energies just above $4m$, corresponding to x just below $x = 0.5$.

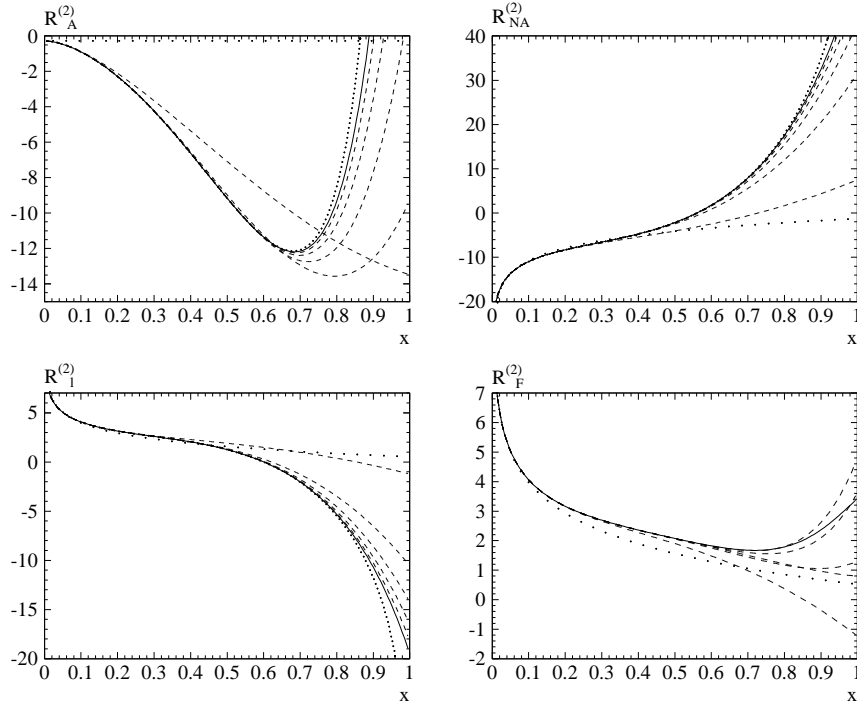


Figure 2: The abelian contribution $R_A^{(2)}$, the non-abelian piece $R_{NA}^{(2)}$, the contribution from light internal quark loops $R_l^{(2)}$ and the contribution $R_F^{(2)}$ from the double-bubble diagram with the heavy fermion in both the inner and outer loop as functions of $x = 2m/\sqrt{s}$. Wide dots: no mass terms; dashed lines: including mass terms $(m^2/s)^n$ up to $n = 5$; solid line: including mass terms up to $(m^2/s)^6$; narrow dots: semi-analytical result (except for $R_F^{(2)}$). The scale $\mu^2 = m^2$ has been adopted.

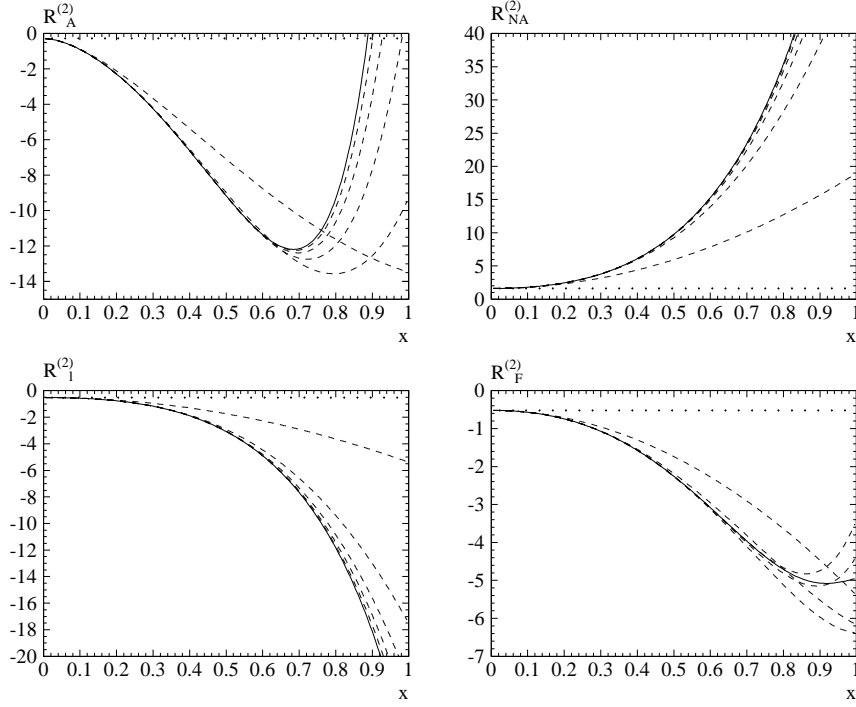


Figure 3: $R_i^{(2)}$, $i = A, NA, l, F$ for $\mu^2 = s$ including successively higher orders in m^2/s . The same notation as in Fig. 2 is adopted. The semi-analytical result is not shown.

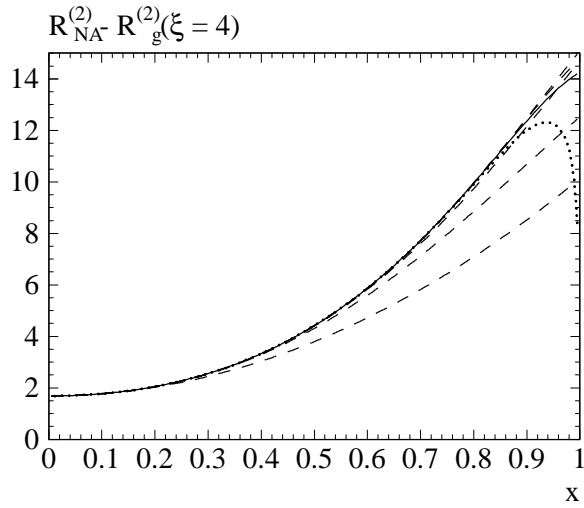


Figure 4: $R_{NA}^{(2)} - R_g^{(2)}(\xi = 4)$ over $x = 2m/\sqrt{s}$. Dotted: semi-analytical result; dashed: mass terms up to $(m^2/s)^5$; solid: mass terms up to $(m^2/s)^6$.

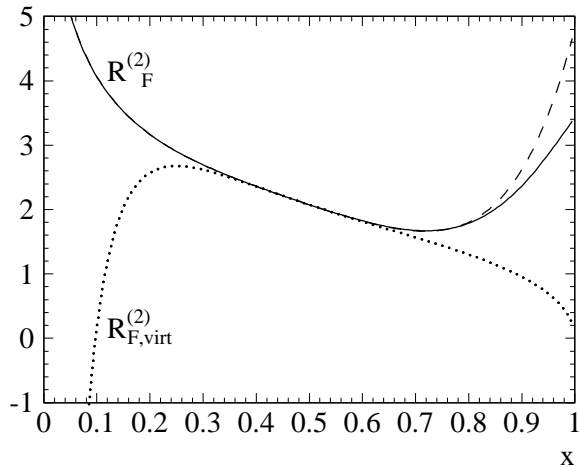


Figure 5: Comparison between the analytical result without 4-particle contribution ($R_{F,virt}^{(2)}$, dotted line) and approximate result with terms up to order $(m^2/s)^5$ (dashed) and $(m^2/s)^6$ (solid line).

Reasonable agreement between the two approaches is therefore expected in the region around $x = 0.5$. This is indeed observed in Fig. 5.

5 Summary

An algorithm has been described which produces the asymptotic expansion of the three-loop vacuum polarization automatically. It generates the relevant subdiagrams and assigns the diagrams automatically to the programs MINCER and MATAD which evaluate the resulting massless propagator and massive tadpole integrals. The output is compared to the quartic terms obtained in [5] and to the semi-analytical results of [8], confirming both these earlier results and the validity of the expansion down to fairly low energy values.

References

- [1] K.G. Chetyrkin, A.L. Kataev and F.V. Tkachov, *Phys. Lett.* **B 85** (1979) 227;
M. Dine and J. Sapirstein, *Phys. Rev. Lett.* **43** (1979) 668;
W. Celmaster and R.J. Gonsalves, *Phys. Rev. Lett.* **44** (1980) 560.
- [2] S.G. Gorishny, A.L. Kataev and S.A. Larin, *Phys. Lett.* **B 259** (1991) 144;
L.R. Surguladze and M.A. Samuel, *Phys. Rev. Lett.* **66** (1991) 560; erratum *ibid.*,
2416;
K.G. Chetyrkin, *Phys. Lett.* **B 391** (1997) 402.

- [3] S.G. Gorishny, A.L. Kataev and S.A. Larin, *Nuovo Cim.* **92A** (1986) 119.
- [4] K.G. Chetyrkin and J.H. Kühn, *Phys. Lett.* **B 248** (1990) 359.
- [5] K.G. Chetyrkin and J.H. Kühn, *Nucl. Phys.* **B 432** (1994) 337.
- [6] A.H. Hoang, J.H. Kühn and T. Teubner, *Nucl. Phys.* **B 452** (1995) 173.
- [7] A.H. Hoang, M. Jezabek, J.H. Kühn and T. Teubner, *Phys. Lett.* **B 338** (1994) 330.
- [8] K.G. Chetyrkin, J.H. Kühn and M. Steinhauser, *Phys. Lett.* **B 371** (1996) 93; *Nucl. Phys.* **B 482** (1996) 213.
- [9] V.A. Smirnov, *Mod. Phys. Lett.* **A 10** (1995) 1485.
- [10] S.G. Gorishny, preprints JINR E2-86-176, E2-86-177 (Dubna, 1986); *Nucl. Phys.* **B 319** (1989) 633;
K.G. Chetyrkin and V.A. Smirnov, preprint INR G-518 (Mocow, 1987);
K.G. Chetyrkin, *Teor. Mat. Fiz* **75** (1988) 26; *ibid.* **76** (1988) 207.
- [11] J.A.M. Vermaseren, *Symbolic Manipulation with FORM*, (Computer Algebra Netherlands, Amsterdam, 1991).
- [12] S.A. Larin, F.V. Tkachov and J.A.M. Vermaseren, Preprint NIKHEF-H/91-18, (1991).
- [13] D.J. Broadhurst, *Z. Phys.* **C 54** (1992) 54.
- [14] K.G. Chetyrkin, R. Harlander, J.H. Kühn and M. Steinhauser, in *Proceedings of the 5th International Workshop on New Computing Techniques in Physics Research: Software Engineering, Neural Nets, Genetic Algorithms, Expert Systems, Symbolic Algebra, Automatic Calculations (AIHENP 96)*, Lausanne, Switzerland, 2–6 September 1996; Report Nos. MPI/PhT/96-122, TTP96-55 and hep-ph/9611354.
- [15] D.J. Broadhurst and S.C. Generalis, Preprint OUT-4102-12, (1984).
- [16] K.G. Chetyrkin and V.P. Spiridonov, *Yad. Fiz.* **47** (1988) 818.
- [17] N. Gray, D.J. Broadhurst, W. Grafe, and K. Schilcher, *Z. Phys.* **C 48** (1990) 673.
- [18] K.G. Chetyrkin, A.H. Hoang, J.H. Kühn, M. Steinhauser and T. Teubner, *Phys. Lett.* **B 384** (1996) 233.